Research Article | Vol. 8, No. 1 | 1 Jan 2018 | OPTICAL MATERIALS EXPRESS 128
Optical Materials EXPRESS

Metamaterial-enhanced terahertz vibrational spectroscopy for thin film detection

JINGYA XIE, XI ZHU, XIAOFEI ZANG, QINGQING CHENG, LIN CHEN, AND YIMING ZHU*

Shanghai Key Lab of Modern Optical Systems, Terahertz Technology Innovation Research Institute, and Engineering Research Center of Optical Instrument and System, Ministry of Education, University of Shanghai for Science and Technology, Shanghai 200093, China
**ymzhu@usst.edu.cn*

Abstract: We present metamaterial-enhanced terahertz vibrational spectroscopy to solve the low sensitivity problem of the THz ray absorption detection in molecular and biomolecular thin film. In a proof-of-principle experiment, we demonstrate the system in split ring resonators (SRRs) metamaterial that is strongly coupled to L-tartaric acid molecular under a low-temperature condition. The experimental results show that the extinction ratio of the detected signal can be significantly improved from 1.75 dB to 4.5 dB. The numerical calculations confirm and explain the experimental observations. By detuning the resonance of metamaterial, the behavior of the spectral signal is modified. When the SRRs and molecular vibrational resonance frequencies are closely aligned, a clear mode splitting is observed resulting in a transparency transmission with enhanced extinction ratio. This method shows great potential for application in thin film sensing by detecting molecular vibrations in the lower-energy terahertz region.

OCIS codes: (160.3918) Metamaterials; (230.5750) Resonators.

References and links

1. B. C. Stipe, M. A. Rezaei, and W. Ho, "Single-molecule vibrational spectroscopy and microscopy," Science **280**(5370), 1732–1735 (1998).
2. K. Liu, M. G. Brown, and R. J. Saykally, "Terahertz laser vibration rotation tunneling spectroscopy and dipole moment of a cage form of the water hexamer," J. Phys. Chem. A **101**(48), 8995–9010 (1997).
3. A. G. Markelz, A. Roitberg, and E. J. Heilweil, "Pulsed terahertz spectroscopy of DNA, bovine serum albumin and collagen between 0.1 and 2.0 THz," Chem. Phys. Lett. **320**(1–2), 42–48 (2000).
4. K. L. Nguyen, T. Friščić, G. M. Day, L. F. Gladden, and W. Jones, "Terahertz time-domain spectroscopy and the quantitative monitoring of mechanochemical cocrystal formation," Nat. Mater. **6**(3), 206–209 (2007).
5. T. Globus, D. Woolard, T. W. Crowe, T. Khromova, B. Gelmont, and J. Hesler, "Terahertz Fourier transform characterization of biological materials in a liquid phase," J. Phys. D Appl. Phys. **39**(15), 3405–3413 (2006).
6. R. Balu, H. Zhang, E. Zukowski, J. Y. Chen, A. G. Markelz, and S. K. Gregurick, "Terahertz spectroscopy of bacteriorhodopsin and rhodopsin: similarities and differences," Biophys. J. **94**(8), 3217–3226 (2008).
7. Z. Jiang, M. Li, and X. Zhang, "Dielectric constant measurement of thin films by differential time-domain spectroscopy," Appl. Phys. Lett. **76**(22), 3221–3223 (2000).
8. S. P. Mickan, K. S. Lee, T. M. Lu, J. Munch, D. Abbott, and X. Zhang, "Double modulated differential THz-TDS for thin film dielectric characterization," Microelectronics J. **33**(12), 1033–1042 (2002).
9. C. Debus and P. H. Bolivar, "Frequency selective surfaces for high sensitivity terahertz sensing," Appl. Phys. Lett. **91**(18), 184102 (2007).
10. G. Ramakrishnan, N. Kumar, P. C. M. Planken, D. Tanaka, and K. Kajikawa, "Surface plasmon-enhanced terahertz emission from a hemicyanine self-assembled monolayer," Opt. Express **20**(4), 4067–4073 (2012).
11. C. Feuillet-Palma, Y. Todorov, A. Vasanelli, and C. Sirtori, "Strong near field enhancement in THz nano-antenna arrays," Sci. Rep. **3**(1), 1361 (2013).
12. Y. M. Bahk, G. Ramakrishnan, J. Choi, H. Song, G. Choi, Y. H. Kim, K. J. Ahn, D. S. Kim, and P. C. Planken, "Plasmon enhanced terahertz emission from single layer graphene," ACS Nano **8**(9), 9089–9096 (2014).
13. S. Bagiante, F. Enderli, J. Fabiańska, H. Sigg, and T. Feurer, "Giant electric field enhancement in split ring resonators featuring nanometer-sized gaps," Sci. Rep. **5**(1), 8051 (2015).
14. L. Xie, W. Gao, J. Shu, Y. Ying, and J. Kono, "Extraordinary sensitivity enhancement by metasurfaces in terahertz detection of antibiotics," Sci. Rep. **5**(1), 8671 (2015).
15. Z. Han, Y. Zhang, and S. I. Bozhevolnyi, "Spoof surface plasmon-based stripe antennas with extreme field enhancement in the terahertz regime," Opt. Lett. **40**(11), 2533–2536 (2015).

#313959 https://doi.org/10.1364/OME.8.000128
Journal © 2018 Received 20 Nov 2017; revised 19 Dec 2017; accepted 19 Dec 2017; published 21 Dec 2017

Optical Materials EXPRESS

16. B. Reinhard, K. M. Schmitt, V. Wollrab, J. Neu, R. Beigang, and M. Rahm, "Metamaterial near-field sensor for deep-subwavelength thickness measurements and sensitive refractometry in the terahertz frequency range," Appl. Phys. Lett. **100**(22), 221101 (2012).
17. X. Wang, C. Luo, G. Hong, and X. Zhao, "Metamaterial optical refractive index sensor detected by the naked eye," Appl. Phys. Lett. **102**(9), 091902 (2013).
18. X. Wu, X. Pan, B. Quan, X. Xu, C. Gu, and L. Wang, "Self-referenced sensing based on terahertz metamaterial for aqueous solutions," Appl. Phys. Lett. **102**(15), 151109 (2013).
19. L. Chen, N. Xu, L. Singh, T. Cui, R. Singh, Y. Zhu, and W. Zhang, "Defect-induced Fano resonances in corrugated plasmonic metamaterials," Adv. Opt. Mater. **5**(8), 1600960 (2017).
20. L. Chen, Y. Wei, X. Zang, Y. Zhu, and S. Zhuang, "Excitation of dark multipolar plasmonic resonances at terahertz frequencies," Sci. Rep. **6**(1), 22027 (2016).
21. H. J. Lee, S. Choi, I. S. Jang, J. S. Choi, and H. I. Jung, "Asymmetric split-ring resonator-based biosensor for detection of label-free stress biomarkers," Appl. Phys. Lett. **103**(5), 053702 (2013).
22. H. J. Lee and J. G. Yook, "Biosensing using split-ring resonators at microwave regime," Appl. Phys. Lett. **92**(25), 254103 (2008).
23. H. Tao, A. C. Strikwerda, M. Liu, J. P. Mondia, E. Ekmekci, K. Fan, D. L. Kaplan, W. J. Padilla, X. Zhang, R. D. Averitt, and F. G. Omenetto, "Performance enhancement of terahertz metamaterials on ultrathin substrates for sensing applications," Appl. Phys. Lett. **97**(26), 4184 (2010).
24. L. Xie, W. Gao, J. Shu, Y. Ying, and J. Kono, "Extraordinary sensitivity enhancement by metasurfaces in terahertz detection of antibiotics," Sci. Rep. **5**(1), 8671 (2015).
25. Z. Chen, R. Mohsen, Y. Gong, T. Chong, and M. Hong, "Realization of Variable Three-Dimensional Terahertz Metamaterial Tubes for Passive Resonance Tunability," Adv. Mater. **24**(23), 143–147 (2012).
26. R. Singh, W. Cao, L. Al-Naib, L. Cong, W. Withayachumnankul, and W. Zhang, "Ultrasensitive terahertz sensing with high-Q Fano resonances in metasurfaces," Appl. Phys. Lett. **105**(17), 171101 (2014).
27. W. Withayachumnankul, J. F. O'Hara, W. Cao, I. Al-Naib, and W. Zhang, "Limitation in thin-film sensing with transmission-mode terahertz time-domain spectroscopy," Opt. Express **22**(1), 972–986 (2014).
28. S. G. Rodrigo, F. J. Garcia-Vidal, and L. Martin-Moreno, "Theory of absorption-induced transparency," Phys. Rev. B **9162**(88), 155126 (2013).
29. J. A. Hutchison, D. M. O'Carroll, T. Schwartz, C. Genet, and T. W. Ebbesen, "Absorption-induced transparency," Angew. Chem. Int. Ed. Engl. **50**(9), 2085–2089 (2011).
30. R. Adato, A. Artar, S. Erramilli, and H. Altug, "Engineered Absorption Enhancement and Induced Transparency in Coupled Molecular and Plasmonic Resonator Systems," Nano Lett. **13**(6), 2584–2591 (2013).
31. J. Xie, X. Zhu, X. Zang, Q. Cheng, Y. Ye, and Y. Zhu, "High extinction ratio electromagnetically induced transparency analogue based on the radiation suppression of dark modes," Sci. Rep. **7**(1), 11291 (2017).
32. R. Nishikiori, M. Yamaguchi, K. Takano, T. Enatsu, M. Tani, U. C. de Silva, N. Kawashita, T. Takagi, S. Morimoto, M. Hangyo, and M. Kawase, "Application of Partial Least Square on Quantitative Analysis of L-, D-, and DL-Tartaric Acid by Terahertz Absorption Spectra," Chem. Pharm. Bull. (Tokyo) **56**(3), 305–307 (2008).
33. Z. Chen, M. Hong, C. Lim, N. Han, L. Shi, and T. Chong, "Parallel laser microfabrication of large-area asymmetric split ring resonator metamaterials and its structural tuning for terahertz resonance," Appl. Phys. Lett. **96**(18), 181101 (2010).
34. K. Chen, R. Adato, and H. Altug, "Dual-Band Perfect Absorber for Multispectral Plasmon-Enhanced Infrared Spectroscopy," ACS Nano **6**(9), 7998–8006 (2012).
35. G. A. Wurtz, P. R. Evans, W. Hendren, R. Atkinson, W. Dickson, R. J. Pollard, A. V. Zayats, W. Harrison, and C. Bower, "Molecular Plasmonics with Tunable Exciton-Plasmon Coupling Strength in J-Aggregate Hybridized Au Nanorod Assemblies," Nano Lett. **7**(5), 1297–1303 (2007).
36. N. T. Fofang, T. H. Park, O. Neumann, N. A. Mirin, P. Nordlander, and N. J. Halas, "Plexcitonic Nanoparticles: Plasmon-Exciton Coupling in Nanoshell-J-Aggregate Complexes," Nano Lett. **8**(10), 3481–3487 (2008).

1. Introduction

Vibrational spectroscopy of molecules is of general importance in chemical and biological identification [1]. In recent decades, terahertz (THz) spectroscopy has received considerable attention, for its energy closing to that of intermolecular interactions, such as hydrogen bonding, the lattice vibration, van der Waals force, and the translational and rotational energy of a molecule [2–4]. Therefore, it is a promising method to measure the spectrum of low-frequency modes of molecules or ensembles, such as crystals and polymers, including proteins, which has proved its effectiveness in detection of skin, breast, liver, colon tumors [5, 6].

A widely applied technique for performing spectroscopic measurements of samples in the THz frequency range is to combine the powdered sample with a binding medium such as polyethylene (PE) powder, such mixture is pressed into a pellet (of the order of 10 mm in diameter), and then placed in the path of the radiation. This technique is simple and well-

Optical Materials EXPRESS

established, but it is not suitable for very small quantities of samples and thin film sensing. Due to the lower interaction between the wave and the molecular/intermolecular vibrational modes in the THz region, detecting molecular vibrations of a thin film is still challenging. To overcome this difficulty, THz differential time-domain spectroscopy was introduced [7, 8]. However, this method needs to restructure the conventional THz time-domain spectroscopy system, which brings extra complexity in system application. Many recent works proposed various micro- and nanostructures, such as a metallic hole array, a ring resonator as well as a spoof surface plasmon based antenna using metal stripes, which are coupled with the THz wave and exhibit near-field enhancement effects [9–20]. A common sensing method using a metamaterial is detecting the resonance shift caused by inducing a change in permittivity of different material on the device [21–27]. This method offers a sensitive approach to molecular detection by revealing the nondispersive component of the material permittivity, yet the molecule vibrational spectroscopy information could not be revealed, which limits its application.

In recent years, absorption-induced transparency (AIT) effect was discovered, which is one of the family of induced transparencies [28, 29]. The most intriguing characteristic of AIT is that the transmission peak, in the combined artificial device plus tested material system, appears at the spectral position where the bare material under test presents resonant absorption. This effect has been demonstrated in the optical frequency range using arrangement metal holes [29] and dipolar rod antennas [30]. However, such effect is not well explored in THz region yet. In this paper, we aim to elucidate enhanced extinction ratio of detected signal for THz spectroscopy application using a simple gold split-ring resonator (SRR) structure based on AIT effect. Not only could such method be used in the nondispersive component of the material permittivity detection, more importantly, when the SRR is tuned to couple with the vibrational mode using AIT effect, the molecule spectroscopy information is revealed. Furthermore, the previous molecule vibrational absorption dip could be transferred into the transmission peak of AIT, which enables larger extinction ratio, hence higher sensitivity. The SRR structure is promising because it is easy to tune the resonant frequency by changing the parameter of the structures. The polarization control of incident wave enables selective excitation of resonances [31]. In a proof-of-principle experiment, we successfully demonstrate metamaterial-enhanced THz spectroscopy of the L-tartaric acid molecule deposited on SRR structures fabricated on a polyimide (PI) substrate. Due to the low absorption in the THz region, the device is measured under low-temperature condition. The results show that the extinction ratio of detected signal can be significantly improved from 1.75 dB to 4.5 dB. This clearly shows the higher sensitivity of this method for the detection of molecules which have the vibrational fingerprints mainly in the THz region. The numerical calculations confirm and explain the experimental observations. We discussed the mechanism by which AIT effect was induced from the viewpoint of the light-matter coupling between the SRR and molecular/intermolecular vibrational modes. When the SRR and molecular vibrational resonance frequencies are closely aligned, a clear mode splitting is observed resulting in a transparency transmission. This kind of resonance shape is easier to identify. Our method can reveal vibrational information of detected material with higher sensitivity and lower system complexity. The results demonstrate the use of THz vibrational sensing for molecules and offer an opportunity to widen the application of THz metamaterials.

2. Device design and fabrication

Schematic presentation of the experiments is shown in Fig. 1(a). We measured the change in spectra of the THz radiation transmitted through the metamaterials following the deposition of L-tartaric acid. The metamaterials consist of metallic arrays of a square SRR with a gap at the center. Here, the resonance of the transmission is determined by the capacitance (C) of the gap structure and the inductance (L) associated with the shape of the square SRR. The L-

Optical Materials EXPRESS

tartaric acid placed on the SRR will cause a near-field coupling, resulting in the spectral change of the resonance in metamaterials. In the coupled system, the resonance mode originates from the SRR, which is induced by the incident wave. Then, the vibrational mode in the L-tartaric acid molecule is coupled with the SRR through near-field coupling, leading to resonance mode hybridization, which is reflected in clear splitting of the fundamental resonances. Therefore, the interference forms a typical AIT system and results in the changing of resonance shape. The device is measured under low-temperature condition of 100K.

Figure 1(b) shows the optical image of the metamaterial with L-tartaric acid deposited on top. The geometric parameters of the optimized unit cell are shown in Fig. 1(c), which are illustrated as follows: all the SRRs are square and the length of their sides is h = 54 μm, the width of metallic arm is w = 6 μm, the size of all the gaps is g = 5 μm. To form a metamaterial structure, the period is P = 60 μm. The total sample array has a footprint of 15 mm × 15 mm = 225 mm^2. The metamaterial sample was fabricated using a surface micromachining process on a polyimide (PI) substrate with thickness of t = 25 μm. A 100 nm-thick gold (Au) with 10 nm of titanium (Ti) film was E-beam evaporated to create the metal film on the substrate. Lift-off of the photoresist was achieved by rinsing in acetone for several minutes and the metal SRRs were formed on the surface of the polyimide. The L-tartaric acid is first dissolved in the alcohol and then dropped on the metamaterial sample, so that it is coated on the metamaterial sample after the alcohol evaporates completely. The thickness of L-tartaric acid film is ~15 μm, which is measured by a stylus profiler.

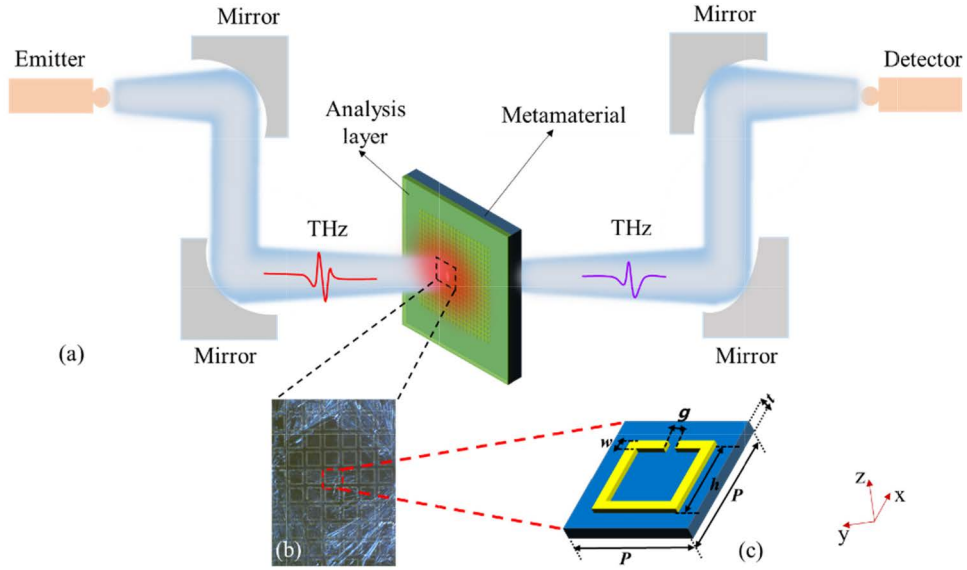

Fig. 1. Schematic illustration of (a) the experiment setup, (b) optical image of the metamaterial with L-tartaric acid deposited on it, and (c) the SRR unit cell.

3. Results and discussions

A conventional THz time-domain spectroscopy system was constructed for the measurement of the extinction spectrum in the THz frequency region with a 9.5 GHz spectral resolution. A femtosecond laser is incident on the photoconductive antenna which emits a linearly polarized THz pulse. The THz radiation from the emitter was collected and focused on the sample with ~1 cm spot diameter by parabolic mirrors. Time traces of the transmitted THz electric field both in amplitude and phase were measured by varying the time delay between the probe beam and the THz pulse. By Fourier transforming the time–domain signal, the amplitude

Optical Materials EXPRESS

spectra were obtained. The extinction spectrum was obtained by recording two spectra of the light transmitted through the sample and through a substrate as a reference. Figure 2(a) presents the simulated transmittance spectra of the SRR metamaterial with the *x*-polarized illumination. The incident electromagnetic wave propagation was normal to the metamaterial. The simulation was performed by solving Maxwell's equations based on the finite element method (FEM). Periodic boundary conditions were used in the *x*- and *y*-directions for simulating an infinite array and port boundary conditions are applied on the top and bottom. The permittivity of the PI substrate was ε_{pi} = 3.5 + 0.01i and the electrical conductivity of gold is $4.561\times10^7 S/m$. The transmittance of the device shows a resonance at 1.14 THz. Figure 2(b) shows the measured transmittance of the fabricated metamaterial with the split gap aligned perpendicular to the electric field of incident wave (*x*-polarized illumination). The discrepancy between the simulated and measured resonances might be due to differences in the SRR structure parameters arising from random fabrication errors.

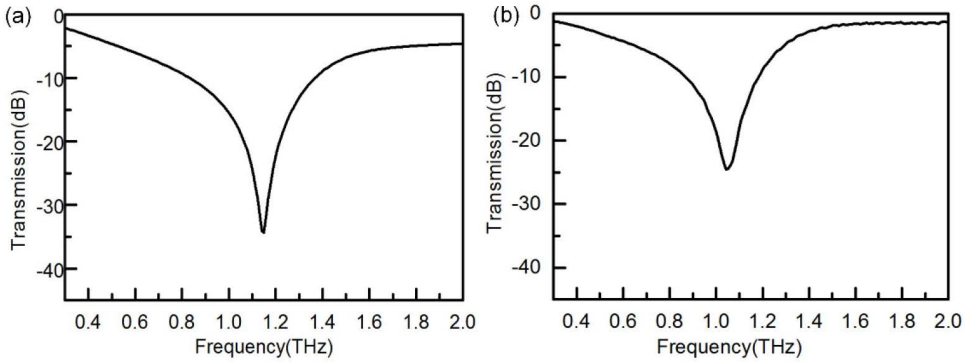

Fig. 2. (a) Simulated transmittance spectra of the SRR metamaterial. (b) Measured transmittance spectra of the fabricated SRR metamaterial.

The pellet under-test was formed by pressing 175 milligrams L-tartaric acid powder. The thickness of pellet is 0.85 mm and its diameter is 13 mm. The absorption spectra of the sample were measured, as shown in Fig. 3. The spectral position and features of the L-tartaric acid signal presented here is close to those described in ref [32]. A blank PI with the identical thickness of the metamaterial was used as a reference, as shown in Fig. 4(a) by the dark-dash curve. The amplitude transmission spectra of 15 μm-thick L-tartaric acid coated on a PI substrate was measured at the temperature of 100 K, which is shown in Fig. 4(a) by the red-dot line. The result shows that a thin layer of L-tartaric acid on the PI substrate displays a weak, broad, and negligibly small signal at the frequency of interest. The blue-solid and green-dash-dot curves present the amplitude transmission of SRR metamaterial with and without 15 μm-thick L-tartaric acid, respectively. There is a clear change of resonance shape. To better reveal and analyze the data, we normalized the transmission as shown in Fig. 4(b). There is a vibrational signal located at 1.035 THz, which is close to bulky pellet samples (1.09 THz). There is a small difference of the vibrational spectra position, since the measurement temperature is reduced from 298 K to 100K to increase the absorption signal of the thin layer of L-tartaric acid. The extinction ratio is the ratio of maximum to minimum transmission power around the resonance, which is defined as 10log10 (P_{high}/P_{low}) [31]. The extinction ratio of the absorption dip is 1.75 dB, as shown in Fig. 4(b) by the dash-blue curve, while the extinction ratio of the transmission peak of AIT is 4.5 dB by the dot-red curve. The sensitivity of detected signal could be characterized by extinction ratio per thickness of material layer. The sensitivity of our method is 0.3 dB/ μm, which is much higher than that of 15 μm-thick L-tartaric acid absorption layer (~0.117 dB/ μm). Hence, such coupling system of the thin layer of L-tartaric acid on the metamaterial exhibits two improved features: the

Optical Materials EXPRESS

extinction ratio of detected signal is strongly enhanced at the identical frequency (from 1.75 dB to 4.5 dB), and there is AIT spectral caused by coupling between the molecular vibration and the electromagnetic resonance of the metamaterial.

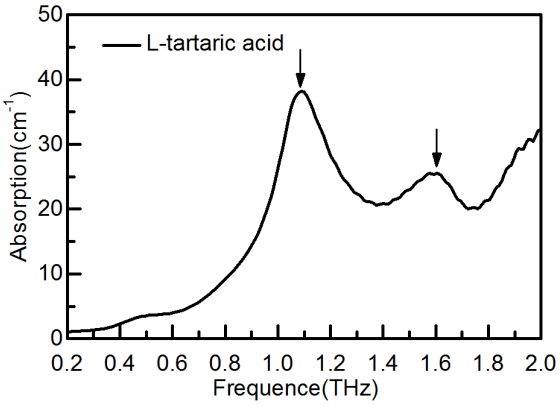

Fig. 3. Absorption spectra of L-tartaric acids.

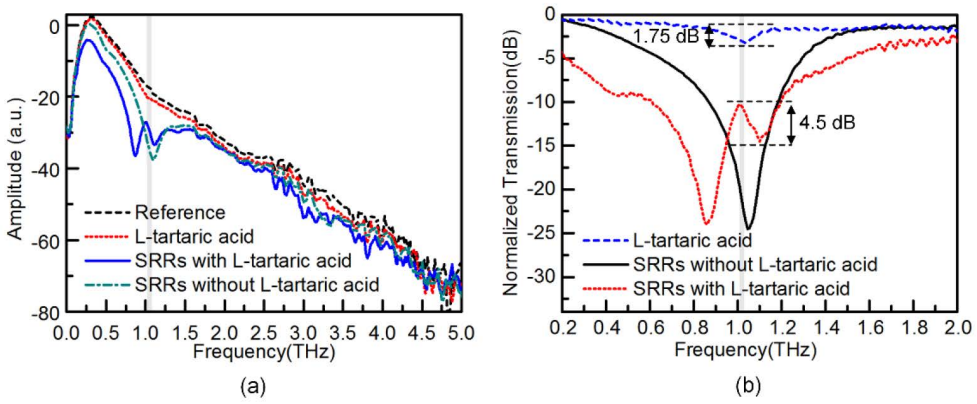

Fig. 4. (a) Frequency-domain transmission spectra of reference and samples. (b) Normalized transmission spectra of samples.

To reveal the underlying mechanism of higher sensitivity and near field coupling characteristics of the L-tartaric acid covered metamaterial sample, we analyzed the dependence of this transmission spectrum. The absorber was modeled as a Lorentz oscillator with permittivity:

$$\varepsilon_{eff} = \varepsilon_{\inf} - \frac{\Delta\varepsilon \cdot f_s^2}{f^2 - f_s^2 + i \cdot f \cdot \Gamma} \tag{1.1}$$

where $\varepsilon_{\inf}$ denotes the off-resonance background permittivity of L-tartaric acid. f_s is the resonance frequency of the transition (absorption peak on the spectral position). Γ is the damping factor. $\Delta\varepsilon$ is the absorption strength. We obtained the resonance frequency f_s=1.035 THz from spectroscopic measurements of L-tartaric acid thin film on the PI substrate. From the spectral width of the absorption line we deduced a damping factor of the resonance Γ_0=170.085 GHz. The absorption strength is fitted to $\Delta\varepsilon$=0.168 . The simulation transmission spectrum of L-tartaric acid thin film on the metamaterial is shown in Fig. 5(a). The period of metamaterial is defined as P = 60 μm. The SRR resonance is then tuned by

Optical Materials EXPRESS

varying the length of SRRs' sides (h). It can also be tuned by varying the gap of SRRs' [33]. As shown in the graph, when the metamaterial resonances are larger than 1.035 THz, the absorption dips appear as red shift; on the other hand, when the metamaterial modes are smaller than 1.035 THz, the dips show blue shift. Such result demonstrates that the spectral shift of the absorption dip is strongly dependent on the spectral position of the metamaterial resonance mode. When the metamaterial and vibrational resonance frequencies are closely aligned, a clear splitting could be observed (brown curve). For each sample, we plot the frequencies of the two dips that result from the interaction between the metamaterial resonance and the vibrational mode against the frequency of the bare metamaterial's initial resonance. The result is shown in Fig. 5(b) as the triangulars and circles. The horizontal pink solid line gives the frequency of the L-tartaric acid band at 1.035 THz, while the blue dashed line is slope = 1, corresponding to the bare metamaterial's resonance frequency. The dark dashed line has a shifted slope to account for the red shifting of the SRR resonance due to the nondispersive component of the L-tartaric acid permittivity, corresponding to ε_{inf}. When detuned from the absorption band, the absorption minima lie at their respective original (noninteracting) positions along the dashed lines. By tuning the resonance frequency of the SRR mode toward that of the absorption band at 1.035 THz, the interaction between the two modes is significantly increased, hence a characteristic mode splitting and anticrossing is observed. As shown in Fig. 5(a), the extinction ratio is also increased with higher interaction strength between the two modes. Similar effects have been found in association with plasmon-exciton coupling in J-aggregate-coated systems at mid-IR [34] and visible frequencies [35, 36]. This enhancement is maximized when the SRR and vibrational resonance are closely aligned. When the clear splitting is observed, the transmission at the SRR resonance dip shows an intense new transmission, resulting in the AIT effect.

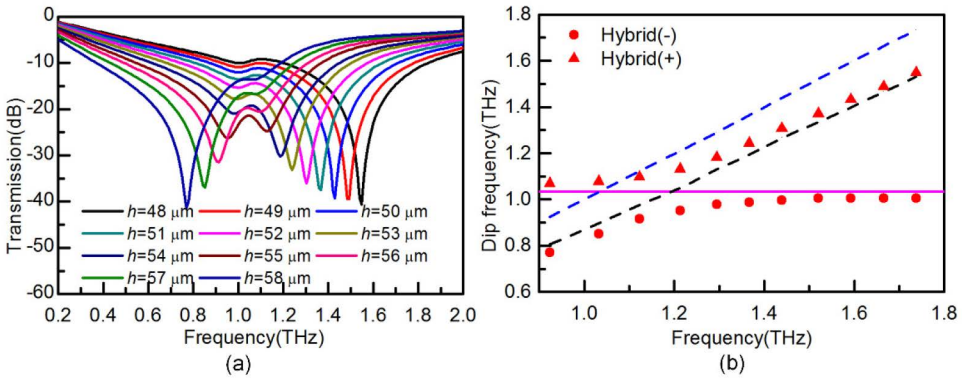

Fig. 5. Coupling between SRR and vibrational modes. (a) Normalized transmission spectra of metamaterial sample coated with L-tartaric acid, which is tuned by varying h. (b) Local minima positions extracted from transmission, plotted against the bare SRR sample's resonant frequencies.

4. Conclusion

In summary, we proposed and experimentally demonstrated that a THz metamaterial with an appropriate design exhibits the molecular vibrational spectroscopy enhancement ability. We show that it can improve the extinction ratio of detected signal from 1.75 dB to 4.5 dB at the resonant frequency. Numerical simulation results indicate that coupling and interference between the electromagnetic resonances in the metamaterial and the molecular vibration are the main mechanisms of signal detection. The present metamaterial-enhanced spectroscopy may be of special use because it offers a simple approach to nondestructively and high-

Optical Materials EXPRESS

sensitivity detecting molecules, which creates a new avenue for adopting THz thin film sensing for industrial applications.

Funding

National Natural Science Foundation of China (61705131, 11604208, 61671302, 61722111); Shanghai Sailing Program (16YF1407900); Natural Science Foundation of Shanghai (16ZR1445500, 16ZR1445600); National Program on Key Basic Research Project of China (973 Program) (2014CB339806); the Major National Development Project of Scientific Instrument and Equipment (2017YFF0106300, 2016YFF0100503); the Key Scientific and Technological Project of Science and Technology Commission of Shanghai Municipality (15DZ0500102); Shanghai Pujiang Program (17PJD028); Shanghai leading talent (2016-019);, and Young Yangtse Rive Scholar (Q2016212).